Construction of Tubular Molecule Aggregations of Graphdiyne for Highly Efficient Field Emission

ARTICLE *in* THE JOURNAL OF PHYSICAL CHEMISTRY C · JANUARY 2011

Impact Factor: 4.77 · DOI: 10.1021/jp107996f

7 AUTHORS, INCLUDING:

Guoxing Li
Pennsylvania State University
15 PUBLICATIONS **427** CITATIONS

SEE PROFILE

Huibiao Liu
Chinese Academy of Sciences
236 PUBLICATIONS **6,334** CITATIONS

SEE PROFILE

THE JOURNAL OF PHYSICAL CHEMISTRY C

ARTICLE

pubs.acs.org/JPCC

Construction of Tubular Molecule Aggregations of Graphdiyne for Highly Efficient Field Emission

Guoxing Li,[†,‡] Yuliang Li,[*,†] Xuemin Qian,[†] Huibiao Liu,[*,†] Haowei Lin,[†,‡] Nan Chen,[†,‡] and Yongjun Li[†]

[†]Beijing National Laboratory for Molecular Sciences (BNLMS), CAS Key Laboratory of Organic Solids, Institute of Chemistry, Chinese Academy of Sciences, Beijing 100190, P. R. China

[‡]Graduate University of Chinese Academy of Sciences, Beijing 100049, P. R. China

Supporting Information

ABSTRACT: Graphdiyne nanotube (GDNT) arrays were prepared through an anodic aluminum oxide template catalyzed by Cu foil. The as-grown nanotubes have a smooth surface with a wall thickness of about 40 nm; after annealing, the GDNTs are about 15 nm. The morphology-dependent field emission properties of graphdiyne arrays were measured and display high performance field emission properties. The turn-on field and threshold field of GDNTs annealed decreased to 4.20 and 8.83 V/μm, respectively.

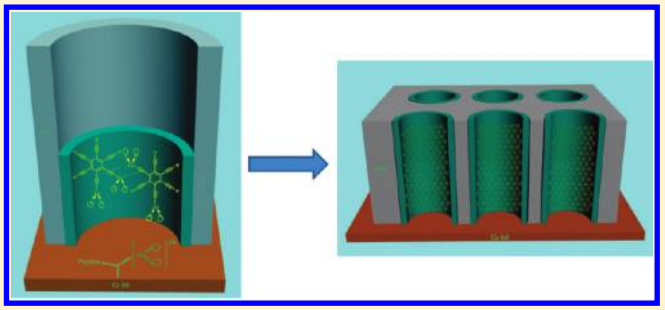

INTRODUCTION

Carbon exhibits a unique ability to form a wide range of structures. During recent years, scientists have synthesized and characterized new carbon allotropes, such as fullerenes,[1] carbon nanotubes,[2] and graphene.[3] Widely recognized as the quintessential nanomaterial, carbon nanotubes have already compiled an impressive list of superlatives since their discovery in 1991. Carbon nanotubes have exhibited good thermal conductivity[4] and outstanding field emission properties.[5] They can also function as the active semiconductor in nanoscale devices,[6] all as a result of their unique topologically controlled electronic properties.[7] Recently, we have successfully prepared a new carbon allotrope—graphdiyne film (GDF) on the surface of copper via a cross-coupling reaction using hexaethynylbenzene, which displayed excellent semiconducting properties.[8] The graphdiyne, which is high conjugated with large diffraction spacing (4.19 Å), chemically stable, and electrically conductive and has the capability to synthesize by chemical methods, is a two-dimensional layer with a one-atom-thick strongly bonded carbon network. The new carbon materials have been proposed for a wide range of promising potential applications in the fields of electronics, semiconductors, and materials.[8,9] Given that one-dimension carbon nanotubes have been employed successfully in the field of nanoelectronics,[10] however, how to produce new and low-dimension nanostructures of graphdiyne materials for future applications in the field of nanoelectronics, this is a significant and ongoing challenge.

In this contribution, we first fabricated the graphdiyne nanotube (GDNT) arrays through association of a template technique and catalyzed cross-coupling reaction. The GDNTs have a smooth surface with a diameter of about 200 nm and a wall thickness of about 40 nm. After annealing at 650 °C for 6 h, the wall thickness of the GDNTs became much thinner, about 15 nm. The field emission properties of GDNT arrays and graphdiyne films were investigated. Annealed GDNT arrays display a turn-on field of 4.20 V/μm, a threshold field of 8.83 V/μm, and work function of 4.29 eV, which exhibits high performance field emission. The field emission stability of GDNT arrays is higher than that of carbon nanotubes and some semiconductors.

EXPERIMENTAL METHODS

Materials and Methods. Unless otherwise stated, reagents and solvents were commercially obtained and used without further purification. Anodic aluminum oxide (AAO) templates with porous diameter of 200 nm and a thickness of 60 μm were purchased from Whatman Co., and the copper foils were pretreated by sonicating in 1 M HCl and acetone and ethanol, sequentially, for 15 min; dried under a flow of argon; and used immediately for preparing graphdiyne nanotubes.

Measurements. The morphologies and energy-dispersive X-ray (EDX) spectrum analysis of the graphdiyne nanotubes were observed on a JEOL JSM 4300F field-emission scanning electron microscope (SEM), at an accelerating voltage of 15 kV. Transmission electron microscopy (TEM) and selected area electron diffraction (SAED) pattern measurements were conducted with JEOL 2010 transmission electron microscopes using an accelerating rate voltage of 120 keV. The X-ray photoelectron spectrometer (XPS) was collected on a VG Scientific ESCALab220i-XL X-ray photoelectron spectrometer using Al Kα radiation as the excitation source. The banding energies obtained in the XPS

Received: August 23, 2010
Revised: November 15, 2010
Published: January 26, 2011

analysis were corrected with reference to C1s (284.8 eV). The Fourier transform infrared (FT-IR) spectrograph was recorded on a Bruker EQUINOX55 FT-IR spectrophotometer. Raman spectra were taken on a Renishaw-2000 Raman spectrometer at a resolution of 2 cm^{-1} by using the 514.5 nm line of an argon ion laser as the excitation source. The field-emission property of GDNT and GDF was measured using a two-parallel-plate configuration in a homemade vacuum chamber at a base pressure of $\sim 1.0 \times 10^{-6}$ Pa at room temperature. The sample was attached to one of two stainless steel plates as a cathode with the other plate as the anode. A dc voltage sweeping from 0 to 3000 V was applied to the sample at a step of 20 V. The emission current was monitored using a Keithley 6485 picoammeter.

Synthesis of Graphdiyne nanotubes. To a solution of 43.6 mg (0.066 mmol) hexakis[(trimethylsilyl)ethynyl]benzene[8] in 15 mL of tetrahydrofuran (THF) was added 0.4 mL of tetra-*n*-butylammonium fluoride (1 M in THF, 0.4 mmol), and the mixture was stirred at 8 °C for 10 min. The solution was then diluted with ethyl acetate, washed with brine, and dried with anhydrous Na_2SO_4. The solvent was removed in vacuo, and the deprotected material (9.08 mg, 62%) was rediluted with 25 mL of pyridine and added slowly to a reactor with 10 mL of pyridine and AAO template, one side of which was fixed on a copper foil at 60 °C under a nitrogen atmosphere. Then the mixture was stirred under a nitrogen atmosphere at 60 °C for 7 days. Upon completion, the AAO template was washed with acetone and DMF in turn, and graphdiyne nanotubes were obtained in the AAO template. Finally, the AAO template was totally solved by NaOH solution (6 M) and washed with ethanol or was selectively etched by NaOH solution (3 M) and cleaned with deionized water for later analysis.

The Annealing Treatment of Graphdiyne Nanotubes. Under a nitrogen atmosphere, the AAO template filled with graphdiyne nanotubes was heated at 650 °C for 6 h. After cooling under the protection of nitrogen, the AAO template was totally solved by NaOH solution (6 M) and washed with ethanol or was selectively etched by NaOH solution (3 M) and cleaned with deionized water for later analysis.

RESULTS AND DISCUSSION

The process and proposed mechanism used to fabricate graphdiyne nanotube arrays is shown in Figure 1. The Cu-pyridine complex was formed in the presence of Cu foil and pyridine, which catalyzed the coupling of alkynyl.[11] Al−O bonds in the AAO template could form the hydrogen bonds with the acetylenic hydrogen of hexaethynylbenzene, resulting in the interaction between hexaethynylbenzene and the active template wall by hydrogen binding. The result led to formation of a film of hexaethynylbenzene deposited on the template wall for inducing the reaction catalyzed by the Cu-pyridine complex in the solution. While the catalytic active center (Cu foil) at the bottom of AAO was covered by the product formed, the Cu-pyridine complex could not be produced to catalyze the cross-coupling reaction sequentially. The reaction was quenched, and the nanotubes were formed on the surface of the template wall. The GDNTs were successfully prepared in the presence of pyridine by a cross-coupling reaction of the monomer hexaethynylbenzene for 7 days at 60 °C under a nitrogen atmosphere.

The morphology of the GDNT array before being annealed was observed by SEM and TEM (Figure 2). Figure 2a shows the top view of the graphdiyne nanotube array. The large number of nanotubes indicated the high filling density of the membrane.

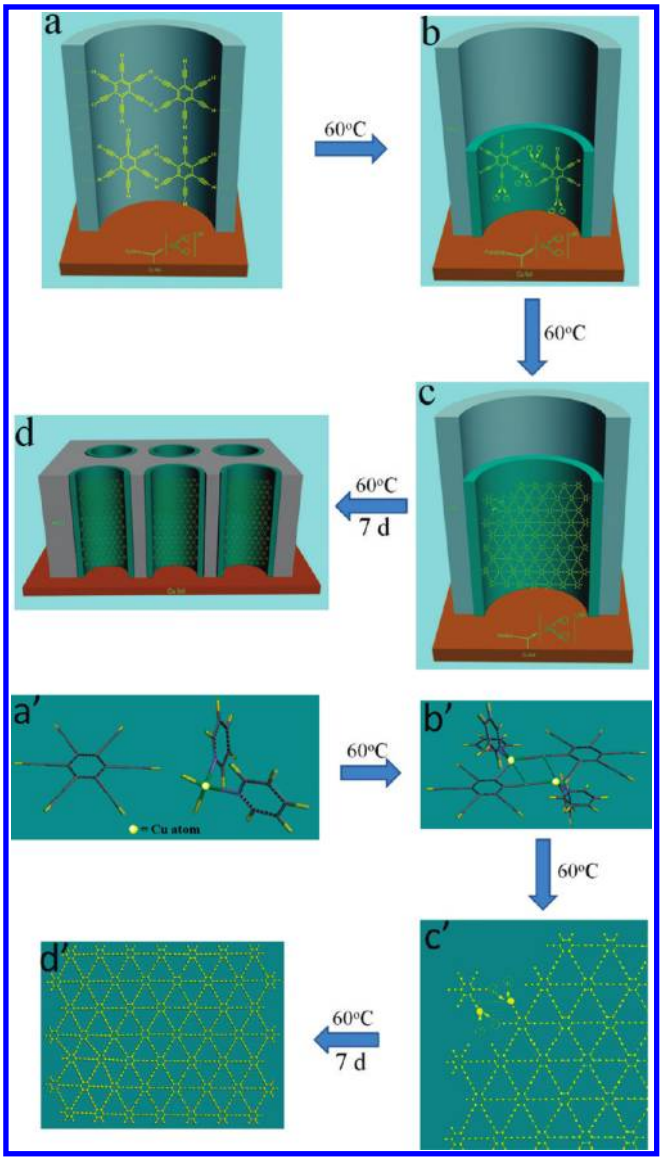

Figure 1. The process (a−d) and proposed mechanism (a′−d′) to fabricate GDNT arrays.

As shown in Figure 2b, the diameter of a GDNT is ~200 nm, and the wall thickness is ~40 nm. The side view of a large area of GDNTs shown in Figure 2c displays that the length of the GDNTs is 40 μm. Figure 2d depicts a side view image of a GDNT array under higher magnification and indicates these nanotubes are well-defined with a smooth surface. Figure 2e and 2f show the TEM images of a GDNT. Figure 2e depicts the bundle of GDNTs, which indicates the tubular structure of the as-prepared nanostructures. The high-magnification TEM image of GDNTs in Figure 2f shows that the nanotube has a smooth surface with a diameter of ~200 nm and the wall thickness is ~40 nm, which agrees well with the SEM images. The SAED pattern shown in the inset of Figure 2f indicates the nanotube is amorphous. The result of EDX spectrum analysis (see the Supporting Information, Figure S1) indicates that the graphdiyne nanotube consists of only elemental carbon.

The morphology of the GDNT array after being annealed at 650 °C for 6 h is shown in Figure 3. Figure 3a−d are SEM images of the GDNT array. We can see the wall thickness of the GDNTs

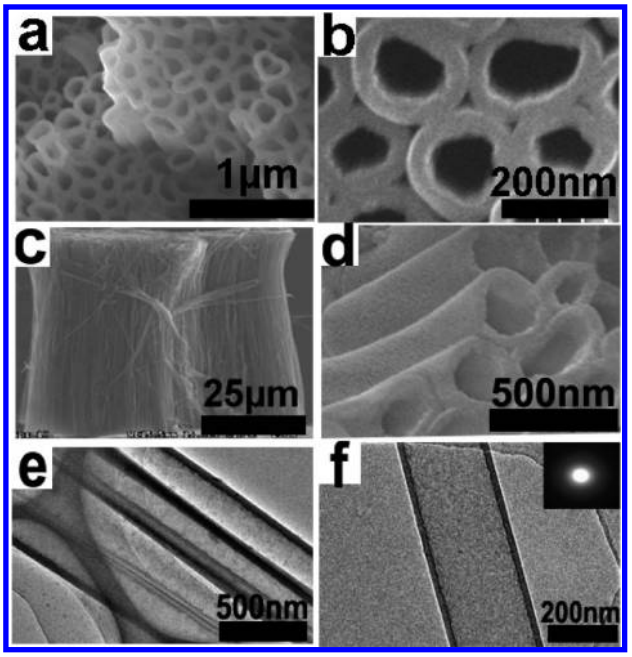

Figure 2. The SEM and TEM images of GDNTs before being annealed: (a) top view of a GDNT array, (b) top view of a GDNT array under higher magnification, (c) side view image of a large area of a GDNT array, (d) side view image of a GDNT array under higher magnification, (e) low-magnification TEM images of a GDNT bundle, and (f) high-magnification TEM images of GDNTs. The inset is the corresponding SAED patterns.

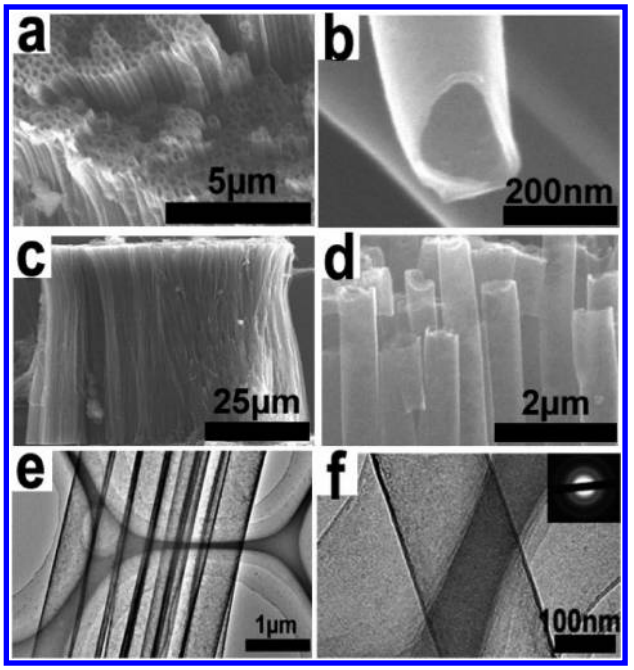

Figure 3. The SEM and TEM images of GDNTs after being annealed: (a) top view of a GDNT array, (b) top view of GDNTs under higher magnification, (c) side view image of a large area of a GDNT array, (d) side view image of a GDNT array under higher magnification, (e) low-magnification TEM images of a GDNT bundle, and (f) high-magnification TEM images of GDNTs. The inset is the corresponding SAED patterns.

became thin, to about 15 nm, and the length did not change. During annealing at 650 °C, the graphdiyne molecules in the GDNT agglomerated and became more compact and orderly, which induced the wall thickness to become thinner. Further structure information and characterization of the GDNTs after being annealed were performed by TEM in Figure 3e−f. Figure 3e indicates the GDNTs have a smooth surface and uniform wall thickness, and the wall thickness became thinner. Figure 3f displays that the wall thickness is ∼15 nm. The SAED in the inset of Figure 3f shows that there are weak polycrystalline rings, which indicates the GDNTs are part crystalline.

The results of XPS (see Supporting Information, Figure S2) are consistent with EDX analysis, indicating unambiguously that GDNTs are composed of only elemental carbon. The C 1s peak at 284.8 eV in Figure S2a shows essentially identical binding energies for the C 1s orbital. The Al 2p peak at 74.6 eV and O 1s peak at 531.9 eV are due to the presence of the AAO template. The absorption of air in graphdiyne nanotubes can contribute in part to the presence of the O 1s. Figure S2b of the Supporting Information presents a high-resolution asymmetric C1s XPS spectrum of graphdiyne nanotubes, and the C 1s peak can be deconvoluted into mainly three subpeaks at 284.5, 285.2, and 287.0 eV, which have been assigned to the C 1s orbital of C−C (sp^2), C−C (sp), and C−O respectively.[8]

Raman spectroscopy was used to evaluate the quality and uniformity of the GDNTs. Figure S3 (see the Supporting Information) shows typical Raman spectra of GDNTs. The Raman spectra display four prominent peaks at 1386.4, 1547.3, 1936.8, and 2183.4 cm^{-1}, respectively. The peak at 1547.3 cm^{-1} corresponds to the first-order scattering of the E_{2g} mode observed for in-phase stretching vibration sp^2 carbon domains in aromatic rings, which is red-shifted compared with the G band of the graphdiyne film (1569.5 cm^{-1}).[8,12] The peak at 1386.4 cm^{-1} is attributed to the breathing vibration of sp^2 carbon domains in aromatic rings, which is a hypsochromic shift compared with the D band of graphdiyne film (1382.2 cm^{-1}).[8,12] The peaks at 2189.8 and 1926.2 cm^{-1} can be attributed to the vibration of conjugated diine links (−C≡C−C≡C−).[8] Figure S4 (see the Supporting Information) shows the FT-IR spectrum of the GDNTs. The typical C≡C stretching vibration band of 2091 cm^{-1} is observed, which is weak because of the molecular perfect symmetry.[8]

The FE measurement of GDNT arrays and graphdiyne film (GDF) were performed. The GDF was prepared according to ref 8. The field emission characteristic of GDNT and GDF are presented in Figure 4. The current density−electric field ($J-E$) curves and the corresponding Fowler−Nordheim (F−N) plots are shown in Figure 4a and b, respectively. For all of the field emission analysis in this study, the turn-on field (E_{to}) and threshold field (E_{thr}) are defined as the electronic fields required to produce a current density of 10 $\mu A/cm^2$ and 1 mA/cm^2, respectively. GDNTs before being annealed exhibit a turn-on field and threshold field of 5.75 and 12.66 V/μm, respectively, and the maximum current density is ∼1.5 mA/cm^2. After being annealed, the field emission property of GDNTs is obviously improved. The turn-on field and the threshold field decreased to 4.20 and 8.83 V/μm, respectively. The maximum current density of GDNT increased to 2 mA/cm^2. The results indicate that the annealing treatment for GDNT enhanced the field emission property.

As demonstrated in Figures 2 and 3, when GDNTs were annealed at 650 °C, the wall thickness decreased to 15 nm, which is about one-third the thickness of the GDNTs before annealing, and the crystallinity of the GDNTs increased. It is well-known

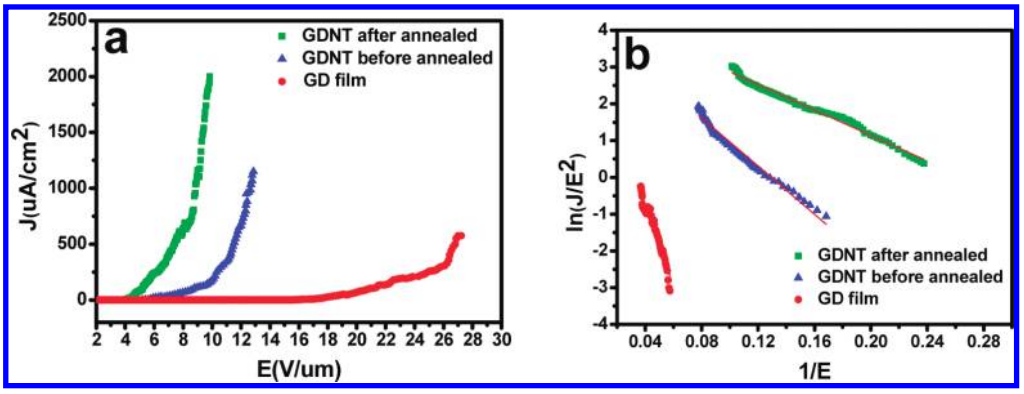

Figure 4. Field emission properties of GDNT array and graphdiyne film: (a) $J-E$ plot of GDNT array before annealing (blue), after annealing (green), and graphdiyne film (red); (b) corresponding $F-N$ plot of GDNT array before annealing (blue), after annealing (green), and graphdiyne film (red).

that the wall thickness is a key factor for nanotube filed emission.[13,14] The thinner wall thickness of a nanotube is favorable to enhancement of the field emission property. The turn-on field and the threshold field of the GDNT after annealing are not only less than that of most organic nanomaterials,[15−21] such as graphene powder, $CuTCNQF_4$, and polydiacetylene nanowires, but also less than that of many inorganic nanomaterials,[13,22,23] such as ZnO, CdS, and CuS. The turn-on field of the GDNTs is higher compared with single-walled carbon nanotubes (1.85 V/μm) and multiwalled carbon nanotubes (2.44 V/μm).[24] Figure 4a shows that the GDFs display a much higher turn-on field of 17.18 V/μm and threshold field of 30.01 V/μm, and the maximum current density is only 0.6 mA/cm^2, which indicates there are morphology-dependent field emission properties.

To further analyze the field emission properties of the GDNT array, the classic F−N law,[25] which was induced on the basis of the electron emission properties from a semi-infinite flat metallic surface, was used to describe the relationship between the J and the local field nearby the emitter.

$$J = E_{loc}^{\ 2} \exp\left(-6.8 \times 10^7 \phi^{3/2}/E_{loc}\right) \quad (1)$$

where J is the current density from the emssion tip, E_{loc} is the local electric field, and ø is the work function of the emitter materials. For an isolated hemisphere model,

$$E_{loc} = V/(\alpha R_{tip}) \quad (2)$$

where V is the applied voltage, R_{tip} is the tip radius of curvature, and α is the modifying factor. From eq 1 and 2, we get

$$\ln(I/V^2) = 1/V\left(-6.8 \times \alpha R_{tip}\phi^{3/2}\right) + \text{offset} \quad (3)$$

$\alpha R_{tip}\phi^{3/2}$ can be estimated from the slope of the F−N plot of $\ln(I/V^2)$ against $(1/V)$. The F−N plots show a linear relationship, implying that a quantum-tunneling mechanism is responsible for the emission. Taking $\alpha = 10$, the R_{tip} of the GDNTs is 15 nm; in our case, the evaluated work function of GDNT is around 4.29 eV,[26,27] which is less than that of graphite (4.9 eV),[28] carbon nanotubes[28], and other carbon nanostructures,[29] demonstrating that the GDNTs have great potential as a competitive candidate for field emitters.

To evaluate the field emission stability of the GNDT arrays, we monitored the current density over 4800 s with starting current densities of 1.3 and 2.5 mA/cm^2, as shown in Figure 5. The observations of the GNDT arrays show that no obvious degradation of current density was detected during a period of 4800 s of

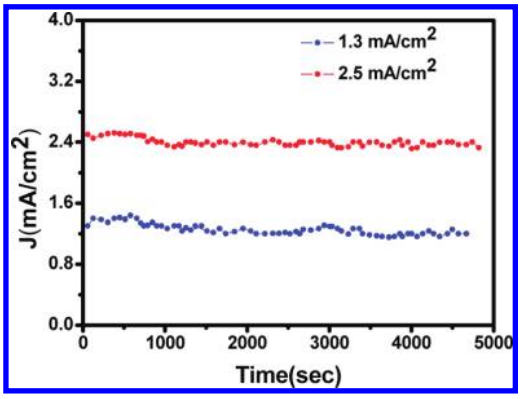

Figure 5. Field emission stability of GDNT arrays.

continuous emission, which demonstrates that GDNT arrays have a high stability of field-emission. The GNDT arrays exhibit better stability than those of carbon nanotubes.[24] The structure stability is the main reason for the excellent field emission stability. Graphdiyne has chemically and physically stable structures and good endurance to the ion bombardment,[9] so there is no obvious degradation of current density.

CONCLUSION

In conclusion, we have demonstrated that GDNT arrays were fabricated by combination of template technique and catalyzed cross-coupling reaction. The FE properties of GDNT arrays and GDF were investigated for the first time. GDNT arrays display excellent field emission properties. The morphology-dependent field emission properties of graphdiyne were observed. The turn-on field and threshold field of annealed GDNTs decreased to 4.20 and 8.83 V/μm, respectively, which are less than that of many semiconductor nanomaterials. GDNTs also exhibited a reduced value of work function and more stability than that of carbon nanotubes. We believe that the novel molecular aggregation of graphdiyne and its outstanding potential properties will guide the development of next-generation electronic and optoelectronic devices, especially vacuum device applications.

ASSOCIATED CONTENT

Supporting Information. EDX analysis, XPS spectra, Raman spectra, and FT-IR spectrum of GDNT. This material is available free of charge via the Internet at http://pubs.acs.org.

AUTHOR INFORMATION

Corresponding Author
*E-mails: (Y.L.) ylli@iccas.ac.cn; (H.L.) liuhb@iccas.ac.cn.

ACKNOWLEDGMENT

This work was supported by the National Nature Science Foundation of China (10874187, 20873155, and 20721061) and the National Basic Research 973 Program of China.

REFERENCES

(1) Krätschmer, W.; Huffman, D. R. *Nature* **1990**, *347*, 354–358.
(2) Iijima, S. *Nature* **1991**, *354*, 56–58.
(3) Novoselov, K. S.; Geim, A. K.; Morozov, S. V.; Jiang, D.; Zhang, Y.; Dubonos, S. V.; Grigorieva, I. V.; Firsov, A. A. *Science* **2004**, *306*, 666–669.
(4) Hone, J.; Batlogg, B.; Benes, Z.; Johnson, A. T.; Fischer, J. E. *Science* **2000**, *289*, 1730–1733.
(5) de Heer, W. A.; Chatelain, A.; Ugaarte, D. A. *Science* **1995**, *270*, 1179–1180.
(6) Collins, P. G.; Arnold, M. S.; Avouris, P. *Science* **2001**, *292*, 706–708.
(7) Hu, J.; Odom, T. W.; Lieber, C. M. *Acc. Chem. Res.* **1999**, *32*, 435–445.
(8) Li, G. X.; Li, Y. L.; Liu, H. B.; Guo, Y. B.; Li, Y. J.; Zhu, D. B. *Chem. Commun.* **2010**, *46*, 3256–3258.
(9) Haley, M. M. *Pure Appl. Chem.* **2008**, *80*, 519–532.
(10) Foldvari, M.; Bagonluri, M. *Nanomed.: Nanotechnol., Biol., Med.* **2008**, *4*, 173–182.
(11) Kennedy, J. C.; MacCallum, J. R.; MacKerron, D. H. *Can. J. Chem.* **1995**, *73*, 1914–1923.
(12) Tuinstra, R.; Koenig, J. L. *J. Chem. Phys.* **1970**, *53*, 1126–1130.
(13) Qian, X. M.; Liu, H. B.; Guo, Y. B.; Zhu, S. Q.; Song, Y. L.; Li, Y. L. *Nanoscale Res. Lett.* **2009**, *4*, 955–961.
(14) Kokkorakis, G. C.; Roumeliotis, J. A.; Xanthakis, J. P. *J. Appl. Phys.* **2004**, *95*, 1468–1472.
(15) Wu, Z. S.; Pei, S. F.; Ren, W. C.; Tang, A. M.; Gao, L. B.; Liu, B. L.; Li, F.; Liu, C.; Cheng, H. M. *Adv. Mater.* **2009**, *21*, 1756–1760.
(16) Liu, H. B.; Zhao, Q.; Li, Y. L.; Liu, Y.; Lu, F. S.; Zhuang, J. P.; Wang, S.; Jiang, L.; Zhu, D. B.; Yu, D. P.; Chi, L. F. *J. Am. Chem. Soc.* **2005**, *127*, 1120–1121.
(17) Liu, H. B.; Wu, X. C.; Chi, L. F.; Zhong, D. Y.; Zhao, Q.; Li, Y. L.; Yu, D. P.; Fuchs, H.; Zhu, D. B. *J. Phys. Chem. C* **2008**, *112*, 17625–17630.
(18) Ouyang, C. B.; Guo, Y. B.; Liu, H. B.; Zhao, Y. J.; Li, G. X.; Li, Y. J.; Song, Y. L.; Li, Y. L. *J. Phys. Chem. C* **2009**, *113*, 7044–7051.
(19) Gan, H. Y.; Liu, H. B.; Li, Y. J.; Zhao, Q.; Li, Y. L.; Wang, S.; Jiu, T. G.; Wang, N.; He, X. R.; Yu, D. P.; Zhu, D. B. *J. Am. Chem. Soc.* **2005**, *127*, 12452–12453.
(20) Cui, S.; Liu, H. B.; Gan, L. B.; Li, Y. L.; Zhu, D. B. *Adv. Mater.* **2008**, *20*, 2918–2925.
(21) Liu, H. B.; Liu, Z.; Qian, X. M.; Guo, Y. B.; Cui, S.; Sun, L. F.; Song, Y. L.; Li, Y. L.; Zhu, D. B. *Cryst. Growth Des.* **2010**, *10*, 237–243.
(22) Qian, X. M.; Liu, H. B.; Guo, Y. B.; Song, Y. L.; Li, Y. L. *Nanoscale Res. Lett.* **2008**, *3*, 303–307.
(23) Fowler, R. H.; Nirdheim, L. W. *Proc. R. Soc. London, A* **1928**, *119*, 173–181.
(24) Jeong, H. J.; Choi, H. K.; Kim, G. Y.; Song, Y. I.; Tong, Y.; Lim, S. C.; Lee, Y. H. *Carbon* **2006**, *44*, 2689–2693.
(25) Collins, P. G.; Zettl, A. *Phys. Rev. B* **1997**, *55*, 9391–9399.
(26) Jonge, N. D.; Allioux, M.; Doytcheva, M.; Kaiser, M.; Teo, K. B. K.; Lacerda, R. G.; Milne, W. I. *Appl. Phys. Lett.* **2004**, *85*, 1607–1609.
(27) Semet, V.; Binh, V. T.; Vincent, P.; Guillot, D.; Teo, K. B. K; Chhowalla, M.; Amaratunga, G. A. J.; Milne, W. I.; Legagneux, P.; Pribat, D. *Appl. Phys. Lett.* **2002**, *81*, 343–345.
(28) Purcell, S. T.; Vincent, P.; Rodriguez, M.; Journet, C.; Vignoli, S.; Guillot, D.; Ayari, A. *Chem. Vap. Deposition* **2006**, *12*, 331–344.
(29) Wu, Y. H.; Yang, B. J.; Zong, B. Y.; Sun, H.; Shen, Z. X.; Feng, Y. P. *J. Mater. Chem.* **2004**, *14*, 469–477.